JOURNAL OF APPLIED PHYSICS **117**, 064104 (2015)

Room temperature nonlinear magnetoelectric effect in lead-free and Nb-doped $AlFeO_3$ compositions

Luiz F. Cótica,[1,2,a)] Guilherme M. Santos,[2] Valdirlei F. Freitas,[3] Adelino A. Coelho,[4] Madhuparna Pal,[1] Ivair A. Santos,[2] Ducinei Garcia,[5] José A. Eiras,[5] Ruyan Guo,[1] and Amar S. Bhalla[1]

[1]*Department of Electrical and Computer Engineering, University of Texas at San Antonio, San Antonio, Texas 78249, USA*
[2]*Department of Physics, State University of Maringá, Maringá – PR 87020-900, Brazil*
[3]*Department of Physics, Universidade Estadual do Centro-Oeste, Guarapuava – PR 85040-080, Brazil*
[4]*Instituto de Física Gleb Wataghin, Universidade Estadual de Campinas, Campinas – SP 13083-859, Brazil*
[5]*Department of Physics, Federal University of São Carlos, São Carlos – SP 13565-905, Brazil*

(Received 16 September 2014; accepted 1 February 2015; published online 10 February 2015)

It is still a challenging problem to obtain technologically useful materials displaying strong magnetoelectric coupling at room temperature. In the search for new effects and materials to achieve this kind of coupling, a nonlinear magnetoelectric effect was proposed in the magnetically disordered relaxor ferroelectric materials. In this context, the aluminum iron oxide ($AlFeO_3$), a room temperature ferroelectric relaxor and magnetic spin glass compound, emerges as an attractive lead-free magnetoelectric material along with nonlinear magnetoelectric effects. In this work, static, dynamic, and temperature dependent ferroic and magnetoelectric properties in lead-free $AlFeO_3$ and 2 at. % Nb-doped $AlFeO_3$ multiferroic magnetoelectric compositions are studied. Pyroelectric and magnetic measurements show changes in ferroelectric and magnetic states close to each other (~200 K). The magnetoelectric coefficient behavior as a function of H_{bias} suggests a room temperature nonlinear magnetoelectric coupling in both single-phase and Nb-doped $AlFeO_3$-based ceramic compositions. © *2015 AIP Publishing LLC*. [http://dx.doi.org/10.1063/1.4908016]

I. INTRODUCTION

Magnetoelectric (ME) materials are characterized by the interactions between magnetic and electric order parameters leading to an electric polarization **P** under application of a magnetic field **H** or a magnetization **M** under application of an electric field **E**.[1] These multifunctional materials open the possibility of electric and magnetic coupling points to integration between ferroelectromagnetic physical properties through the ME effects to promote interesting technological advances in many electronic devices.[2,3] Although Dzyaloshinskii described the magnetoelectric effect in 1959,[4] finding novel technologically useful materials displaying strong ME coupling at room temperature remains a challenging problem.[5] This is mainly because there are few single-phase materials in nature that possess both ferroelectric and magnetic properties independently and the occurrence of linear magnetoelectricity is very rare because of its high symmetry demands.[1]

In addition, despite the fact that single-phase systems are more interesting for large scale production, until now, with exception of $BiFeO_3$ and $BiFeO_3$-based compositions,[6–8] most reported single-phase materials demonstrate linear ME coupling only at very low temperatures.[9,10] Such reported materials include the linear ME coupling in lead-free based bulk materials.[11]

Due to the fact that few single-phase materials present ME coupling at room temperature, the search for new materials with such capabilities should consider further possibilities. For example, magnetically frustrated systems have been identified to possess magnetoelectric effects at low temperature. As an example, $MnWO_4$ shows strong temperature and external magnetic field dependence of its ferroelectric loops.[12] Similarly, high-temperature multiferroic behavior has been studied in $PbFe_{0.5}Ti_{0.5}O_3$ and in $PbFe_{2/3}W_{1/3}O_3$/$PbTiO_3$.[13,14]

In addition to the magnetically frustrated systems, nonlinear magnetoelectric effects have been proposed in materials where magnetically disordered (magnetic spin glass) and relaxor ferroelectric states coexist.[15] Relaxors are materials with short-range polarization ordering and highly frequency dependent dielectric properties.[16] In analogy, a magnetic spin glass (a relaxor ferromagnet) is expected to have no long-range magnetic order, exhibiting a high value of the quasistatic magnetic response in a broad temperature range, strong frequency dispersion, as well as a Vogel-Fulcher-type freezing of the dynamic magnetic response.[17]

In this scenario, the aluminum iron oxide ($AlFeO_3$), a room temperature ferroelectric relaxor (T^m[1 kHz] = 230 K) and magnetic spin glass (T^m[1 kHz] = 240 K) compound, emerges as a new single-phase lead-free material that can exhibit magnetoelectricity at room temperature.[18–21] This material has an orthorhombic symmetry ($Pna2_1$ space group—see Figure 1(a)),[18,21] presents a complex magnetic freezing at temperatures below 220 K, and a ferroelectric ordering close to the magnetic transition.[18,20–22] These complex behaviors come from four different cation sites named Fe1, Fe2 (predominantly occupied by iron—Figure 1(b)) and

a)Author to whom correspondence should be addressed. Electronic mail: lfcotica@dfi.uem.br. Tel.: +5544-3011-5904. Fax: +5544-3263-4623.

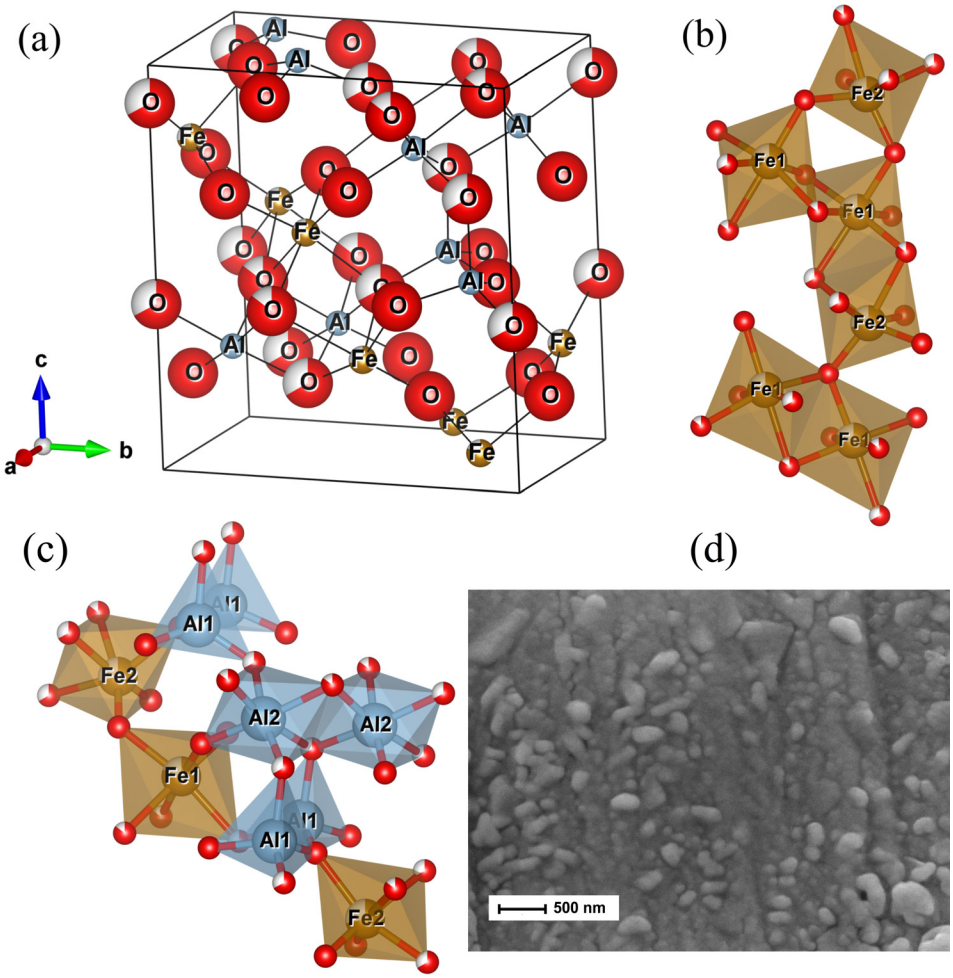

FIG. 1. (a) Orthorhombic symmetry ($Pna2_1$ space group) of $AlFeO_3$ unit cell. (b) Fe1 and Fe2 sites, predominantly occupied by iron. (c) Al1 and Al2 sites, predominantly occupied by aluminum. The oxygen environment of these cation sites is octahedral except the Al1 site, which is tetrahedral. (d) Surface Scanning Electron Microscopy image for AFO-2N ceramic.

Al1 and Al2 (predominantly occupied by aluminum—Figure 1(c)). The oxygen environment of these cations is octahedral except for the Al1 site, which is tetrahedral.[18,21,22] To the best of our knowledge, there is no direct evidence of a ME coupling in any $AlFeO_3$ (AFO) composition in the literature until now. This paper aims to show and discuss static, dynamic, and temperature dependent ferroic and magnetoelectric properties in $AlFeO_3$ based materials. The main objective is to investigate the coupling of the magnetic and electrical order parameters in $AlFeO_3$ compositions.

II. EXPERIMENTAL

Experimental procedures to obtain AFO and 2 at. % Nb-doped $AlFeO_3$ (AFO-2N) composition powders have been discussed in previous works.[18,21] The resulting powders were pressed into disc form (5 mm of diameter and 1 mm of thickness) and sintered at 1700 K for 10 h in an O_2 atmosphere (1 atm). The relative ceramic densities were calculated as being ~95%. In order to obtain microstructural information, scanning electron microscopy (SEM) images were obtained in a Shimadzu Super Scan SS-550 microscope. Gold electrodes were sputtered on ceramic surfaces across the thickness direction prior to electric and magnetoelectric characterizations.

Zero field cooling DC magnetization measurements were performed using a Quantum Design MPMS-5S SQUID magnetometer. Computer assisted pyroelectric measurements were carried out by using an HP 4140B pA meter at a constant rate of $2\,K\cdot min^{-1}$ of a sample in a closed cycle cryostat (Sumitomo cryogenics) and a Lake Shore 331 temperature controller. In both pyroelectric and magnetoelectric measurements, voltage (100 V) was applied to the samples during the cooling process by using a power supply. In order to achieve ME voltage effect, the samples were exposed to both AC magnetic field ($h_{ac} = 1$–20 Oe at 100 Hz–10 kHz) and bias DC magnetic field (H_{bias}). The h_{ac} field was produced by a digital function generator driven Helmholtz coils. Custom-built Helmholtz coils were placed inside the cryostat vacuum chamber. The H_{bias} field was generated by a DC electromagnet powered by a bi-polar power supply. The ME voltage response was then measured through a SR850 digital lock-in amplifier, the h_{ac} strength was obtained by the electric current measurement in the Helmholtz coils using a 6–1/2 digit precision multimeter (Fluke 8845A) and the H_{bias} strength was recorded by using a Walker Scientific Inc. MG-4D gaussmeter. The magnetic fields were applied parallel to each other and perpendicular to the sample plane. The sample cooling was regulated by a LakeShore 331 temperature controller and generated by a closed cycle cryostat. Measurements were then recorded via interfacing with a computer system. The ME voltages were measured as a function of field intensity (h_{ac} and H_{bias}), frequency, and temperature.

III. RESULTS AND DISCUSSION

Structural properties of AFO and AFO-2N have been carefully studied and published elsewhere.[18,20,21] Both compositions, AFO and AFO-2N, are crystallized in an orthorhombic symmetry (Figures 1(a)–1(c)). Figure 1(d) shows a surface SEM image for AFO-2N (AFO sample revealed quite similar images—not shown). The microstructural studies revealed dense ceramics with sintered grains in a size distribution between 100 nm and 500 nm.

Figures 2(a) and 2(b) show the pyroelectric measurements for AFO and AFO-2N ceramics, respectively. In both the figures, the temperature dependence of the pyroelectric coefficient (p) and the electric polarization (ΔP) is shown. The pyroelectric depolarization current was obtained on heating the sample at a constant rate of 2 K min^{-1} from 100 to 260 K on a pre-poled sample at 100 K. The temperature dependence of pyroelectric coefficient was obtained using the relation

$$p = \frac{i}{sb}, \tag{1}$$

where p is the pyroelectric coefficient, i is the depolarization current, s is the area of the electrode, and $b = d\mathrm{T}/d\mathrm{t}$ is the heating rate. The electric polarization ΔP was calculated using the integral relationship

$$\Delta P = \int p dT. \tag{2}$$

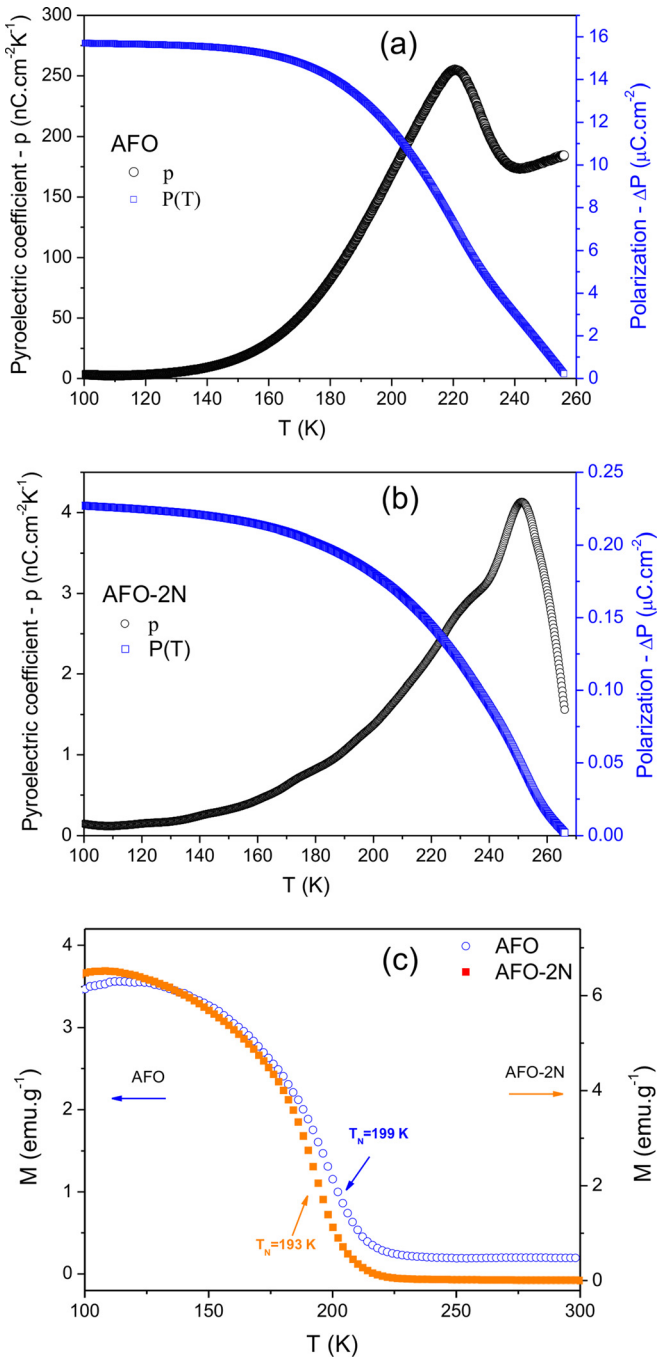

FIG. 2. Pyroelectric measurements in (a) AFO and (b) AFO-2N ceramics: pyroelectric coefficient (blue), p, and polarization (black), ΔP, as a function of temperature. (c) Temperature dependence of AFO and AFO-2N samples magnetization (M) under a zero field cooling protocol with a 0.02 T applied field.

Peaks can be seen in the pyroelectric coefficient curves at 220 K (AFO) and 253 K (AFO-2N). These peaks are due to the depolarization and are indicative of a ferroelectric state change (a freezing process) both in AFO and AFO-2N. At 160 K, the pyroelectric coefficient was found to be $p = 30$ nC cm^{-2} K^{-1} and the polarization, $\Delta P = 15$ μC cm^{-2} for AFO. At same temperature, for AFO-2N, $p = 3.8$ nC cm^{-2} K^{-1} and $\Delta P = 0.4$ μC cm^{-2}. The AFO ΔP values are much higher than those shown by Saha *et al.* for $AlFeO_3$ and $GaFeO_3$, while the AFO-2N ΔP values are very close to those values reported by Saha *et al.*[23] Perhaps this difference in ΔP values may be attributable to differences in samples' quality.

The observed behaviors (Figs. 2(a) and 2(b)) are in agreement with dielectric permittivity and loss tangent measurements already published.[21] Also, the dielectric permittivity studies revealed an underneath relaxor-like behavior, since ε_r *vs* T dispersion follows an Arrhenius-like behavior, and Vogel-Fulcher temperatures (T_{VF}) of ~150 K and ~200 K for AFO and AFO-2N, respectively.

The temperature dependence of the samples magnetization (M), in a zero field cooling protocol with a 0.02 T applied field, is shown in Figure 2(c). The curves suggest a magnetic transition for a ferrimagnetically ordered state at about 199 K and 193 K for AFO and AFO-2N, respectively, with an elevated magnetization in comparison to other multiferroic magnetoelectric materials.[21] Santos *et al.*,[21] by using magnetic AC susceptibility measurements, showed peaks with the temperature of maximum susceptibility (T^m) close to those observed in Figure 2(c). These peaks confirm the transition from a (super)paramagnetic-like state (glassy state) to a frozen magnetic state, when the temperature is decreased. Also, it was identified that the frequency dependence of T^m follows a Vogel-Fulcher law for AFO, suggesting a classical spin glass behavior; however, a similar behavior was not clearly observed in AFO-2N.

The results presented in Figure 2 suggest a close correlation between the magnetic and ferroelectric domains in $AlFeO_3$-based compositions. In fact, when the magnetic spin-glass components slow down, the frozen ferroelectric glassy response peaks up as indicated by pyroelectric activity

and by the relaxor behavior of the AFO and AFO-2N samples.[21] To clarify a possible coupling between magnetic and ferroelectric states, a detailed study of the magnetoelectric effect in these samples has been performed.

The ME coefficient as a function of H_{bias} can be seen in Figures 3(a) and 3(b) for AFO and AFO-2N, respectively. First, before beginning the measurements, the samples were subjected to a high field condition ($H_{bias} = 3.5$ kOe) until the voltage output reached equilibrium. Subsequently, the dynamic measurements were performed initially by decreasing H_{bias} from +3.5 kOe to −3.5 kOe and, then, returning to $H_{bias} = +3.5$ kOe. In both the samples, it is possible to obtain a hysteretic behavior probably due to a remnant magnetic field. On the other hand, the observed behavior cannot be associated with a linear magnetoelectric effect but can be attributed to a non-linear magnetoelectric coupling, i.e., the ME coupling observed in AFO and AFO-2N at room temperature presents a more complex interaction between the magnetostrictive and electrostrictive coefficients similar to those shown by Shen *et al*. and Blinc *et al*.[15,24,25] Blinc *et al*. also showed that this nonlinear effect could happen in materials which exhibit ferroelectric relaxor and magnetic spin glass behavior within the same temperature range.[15] In fact, they showed that the polarization of a polar nanoregion (locally ferroelectrically ordered structures) can be nonlinearly increased by applying an external magnetic field (H^{ext}). Actually, such systems have strong fourth-order ME coupling in the free energy of E^2H^2 type.[15] Consequently, in our work, by applying external magnetic fields (H_{bias} and h_{ac}), the polarization of polar nanoregions in both AFO and AFO-2N was increased leading to the nonlinear ME behavior as presented in Figure 3. At 100 K, as expected, when AFO and AFO-2N are no longer in the ferroelectric relaxor and magnetic spin glass states, due to the freezing of electric and magnetic moments, the nonlinear ME effect is significantly reduced leading to a lowering of the ME coefficient in both AFO (Figure 3(c)) and AFO-2N (Figure 3(d)) samples. In fact, at low temperatures, the linear ME coupling seems to be dominant.

Furthermore, it is also interesting to note in the magnetoelectric measurements that, due to the nonlinear behavior of ME coupling, two regions with different slopes were observed in the studied samples. The first effect occurs when the measurements start at high values of H_{bias} (3.5 kOe), as in Figure 3. A second behavior was observed when the samples were subjected to low field measurements (starting $H_{bias} = 1.3$ kOe). In this regime, the ME coefficient reached a maximum at very low values of H_{bias} (Figure 4). At 300 K, the ME coefficient reached the maximum value at $H_{bias} = 160$ Oe (5.46 mV cm^{-1} Oe^{-2}), for AFO, and $H_{bias} = 10$ Oe (5.40 mV cm^{-1} Oe^{-2}), for AFO-2N. At 100 K, the maximum in the ME response is shifted for even lower H_{bias} values in both AFO (10 Oe–2.62 mV cm^{-1} Oe^{-2}) and AFO-2N (2 Oe–1.42 mV cm^{-1} Oe^{-2}). In fact, these behaviors are well understood when compared with typical magnetostrictive measurements. Although no magnetostriction measurements in $AlFeO_3$-based compositions are performed here, we believe the magnetostrictive behavior in these materials is close to the nonlinear magnetoelectric behavior.[24]

Figure 5 shows the ME response as a function of frequency (100 Hz to 10 kHz), h_{ac} (1–20 Oe), and temperature (300 K and 100 K) for AFO and AFO-2N ceramics. The measurements were performed by using $H_{bias} = 0$ and $H_{bias} = 2.5$ kOe. As can be seen in all the measurements, the effect of H_{bias} was very small and hence Figure 4 shows such representative results measured only for $H_{bias} = 2.5$ kOe.

In Figures 5(a) and 5(b), it can be seen that the ME coefficient increases in both the samples with increasing frequency at 300 K as well as 100 K. The ME coefficient reaches 17.4 mV cm^{-1} Oe^{-2} for AFO and 12.7 mV cm^{-1}

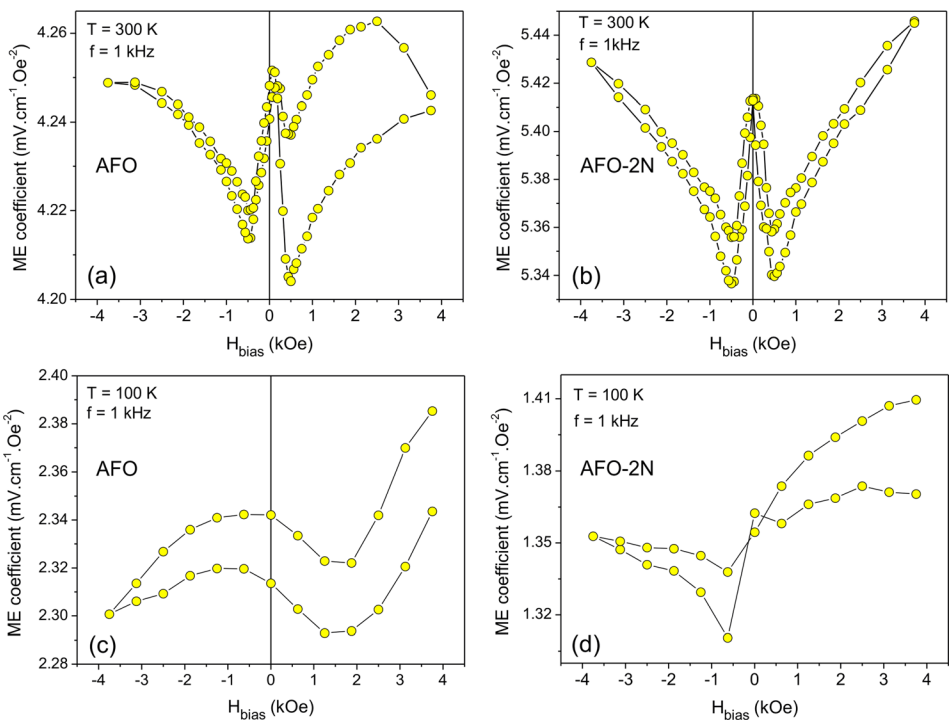

FIG. 3. The ME coefficient as a function of H_{bias} for AFO ((a) T = 300 K and (c) T = 100 K) and AFO-2N ((b) T = 300 K and (d) T = 100 K).

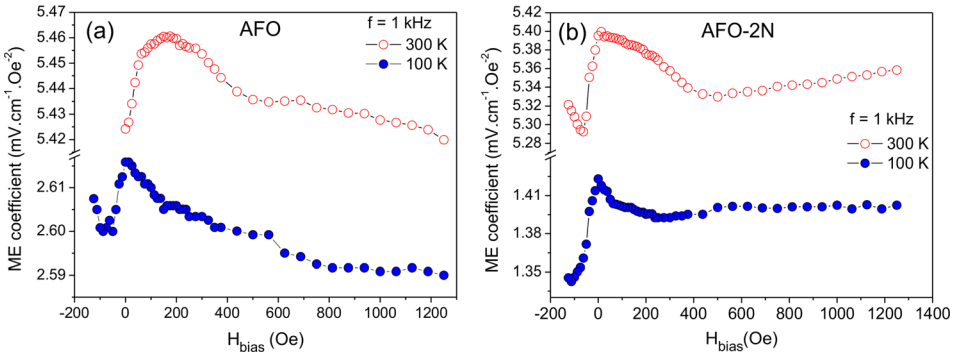

FIG. 4. Low field measurements of the ME coefficient as a function of H_{bias} for (a) AFO and (b) AFO-2N.

Oe^{-2} for AFO-2N at 10 kHz and 300 K. In addition, a significant reduction in the ME response occurs at 100 K, again indicating the nonlinear behavior in the magnetoelectric effect, mainly for AFO-2N. In effect, at 100 K both ferroelectric and magnetic nanodomains are frozen. The evidence from the data suggests a dynamic coupling between magnetic and ferroelectric states. Indeed, such an interaction is further reinforced by the data at 300 K since both magnetic and ferroelectric states are glassy states and the magnetoelectric effect is amplified.

Regarding the ME response as a function of h_{ac} intensity while keeping f = 1 kHz, i.e., the induced electric field inside the sample due to an external AC magnetic field (Figures 5(c) and 5(d)), in both the samples the induced response increases linearly with the increasing intensity of h_{ac}. At $h_{ac} = 20$ Oe (300 K), the ME output reaches 108.4 mV cm^{-1} for AFO and 107.7 mV cm^{-1} for AFO-2N. A significant decrease in the ME response value is observed at 100 K in both the samples and exhibits a similar trend as in the frequency dependent measurements.

The magnetoelectric effect results presented in Figures 3–5 suggest that in addition to the results presented on AFO previously,[21] the magnetic behavior of AFO-2N is also a spin-glass like state. This can be concluded using the fact that AFO-2N presents very similar magnetoelectric behavior as that of pure AFO, i.e., both systems present a nonlinear magnetoelectric behavior and, consequently, both should be in ferroelectric relaxor and magnetic spin glass states having magnetic T_{VF} and ferroelectric T_{VF} close within the similar temperature range.

In order to explain the possible origin of the observed ferroelectric, magnetic, and magnetoelectric states, a careful study in the room temperature $AlFeO_3$ structural arrangement was performed. By employing structural parameters obtained in previous works, we can provide details about the Fe1, Fe2, Al1, and Al2 sites (Figure 6(a)).[18,21,22] It is easy to show that the central atoms of Fe1 and Fe2 sites are off-centered. Consequently, these sites should have polar regions that result in or provide ferroelectric properties to the whole material. Similar features are less pronounced in Al1 and Al2 sites. Concerning the magnetic properties and differently than that proposed by Bouree *et al.*,[22] the main resultant magnetization probably comes from a super-exchange interaction between Fe1 and Fe2 sites across the

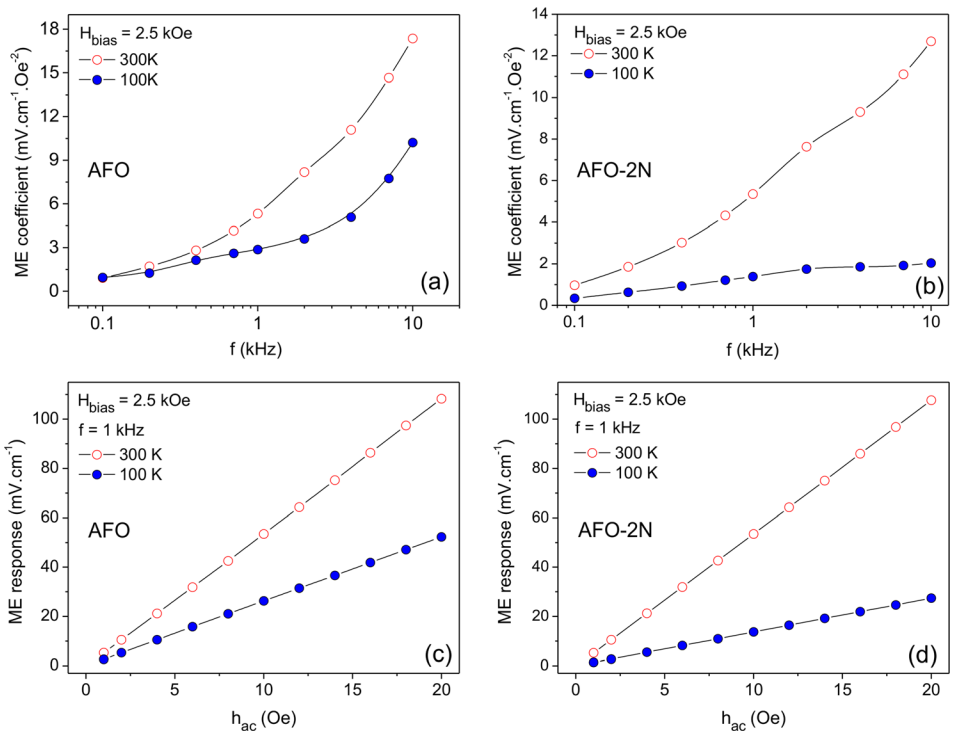

FIG. 5. ME response as a function of frequency (100 Hz to 10 kHz), h_{ac} (1-20 Oe), and temperature (300 K and 100 K) for AFO ((a) and (c)) and AFO-2N ((b) and (d)) ceramics.

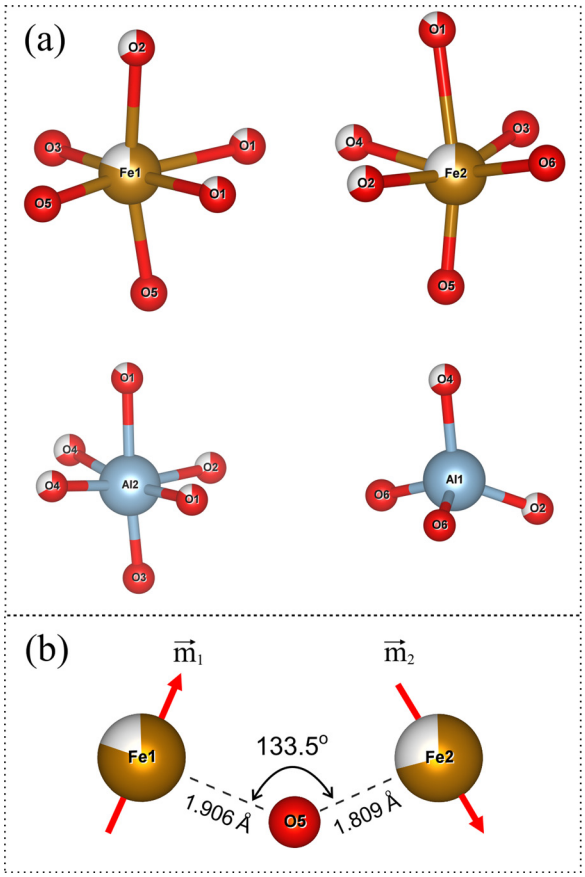

FIG. 6. (a) Room temperature structural arrangement for Fe1, Fe2, Al1, and Al2 sites in $AlFeO_3$. (b) Superexchange interaction between Fe1 and Fe2 sites across the O5 site. Due to the strong "180° cation-anion-cation" superexchange antiferromagnetic interactions, the Fe^{3+} cations Fe1 and Fe2 have their spins oppositely oriented, except for the angle shown in the figure.[22]

O5 site (Figure 6(b)). As the iron fractions are different in each site (0.78 for Fe1 and 0.76 for Fe2), the antiferromagnetic superexchange interaction leads to a classical Néel ferrimagnetism.[22,26]

As can be observed in Figure 6, the O5 site connects Fe1 and Fe2 sites and also connects the octahedral environments. As a consequence, the magnetoelectric coupling probably comes from this connection.[27] Here, we suggest that new experimental and theoretical studies that probe this environment can elucidate the origin of the coupling between magnetic and ferroelectric properties in $AlFeO_3$-based compositions.

In summary, a room temperature nonlinear magnetoelectric coupling is evident in single-phase $AlFeO_3$-based ceramic compositions. This makes the AFO-based compositions an important family of lead-free multiferroic materials, which can be further investigated for possible multifunctional device applications. Besides that, opportunities for more fundamental, theoretical, and experimental studies mainly focusing on the origin of the coupling between ferroelectric and magnetic properties in these materials are opened up. As an additional advantage to the study of AFO-based compositions, these materials offer a lower environmental impact and higher spontaneous magnetization in comparison to other lead-based multiferroics, facilitating attractive technological applications.

IV. CONCLUSIONS

In this work, static, dynamic, and temperature dependent ferroic and magnetoelectric properties in the lead-free $AlFeO_3$ and 2 at. % Nb-doped multiferroic magnetoelectric compositions were studied. Pyroelectric and magnetic measurements show ferroelectric (T_{VF}—freezing) and magnetic states transitions within the same temperature range (~200 K). The magnetoelectric voltage response as a function of H_{bias} suggests a room temperature nonlinear magnetoelectric coupling in both single-phase $AlFeO_3$-based ceramic compositions. Due to the fact that very few single-phase materials exhibit magnetoelectric effects at room temperature, this family of materials becomes an important multiferroic family to be investigated for potential device applications. Additionally, these materials offer a lower environmental impact (lead-free) and higher spontaneous magnetization in comparison to other lead-based multiferroics. Hence, these materials may be fascinating for several technological applications. Finally, the origin of the coupling between ferroelectric and magnetic properties and the connection between Fe1 and Fe2 sites should be further investigated to better understand the mechanisms that provide these enhanced room temperature magnetoelectric properties. The improved fundamental understanding of these materials may lead to further enhancement of lead-free magnetoelectric properties and improved devices.

ACKNOWLEDGMENTS

The authors would like to thank the Brazilian agencies CNPq (proc. 305129/2010-4), FAPESP (proc. 2008/04025-0), Fundação Araucária de Apoio ao Desenvolvimento Científico e Tecnológico do Paraná (Prots. 22825 and 22870), and CAPES (PROCAD 082/2007) for financial support. L.F.C. also acknowledge UTSA under the INAMM/NSF program for hosting him.

[1]N. A. Hill, J. Phys. Chem. B **104**, 6694 (2000).
[2]K. Ueda, H. Tabata, and T. Kawai, Appl. Phys. Lett. **75**, 555 (1999).
[3]M. M. Kumar, M. B. Suresh, S. V. Suryanarayana, G. S. Kumar, and T. Bhimasankaram, J. Appl. Phys. **84**, 6811 (1998).
[4]I. E. Dzyaloshinskii and L. P. Pitaevskii, Sov. Phys. JETP - USSR **9**, 1282 (1959).
[5]M. Fiebig, J. Phys. D: Appl. Phys. **38**, R123 (2005).
[6]V. F. Freitas, L. F. Cotica, I. A. Santos, D. Garcia, and J. A. Eiras, J. Eur. Ceram. Soc. **31**, 2965 (2011).
[7]L. F. Cotica, F. R. Estrada, V. F. Freitas, G. S. Dias, I. A. Santos, J. A. Eiras, and D. Garcia, J. Appl. Phys. **111**, 114105 (2012).
[8]R. A. M. Gotardo, L. F. Cotica, I. A. Santos, M. Olzon-Dyonisio, S. D. Souza, D. Garcia, J. A. Eiras, and A. A. Coelho, Appl. Phys. A: Mater. Sci. Process. **111**, 563 (2013).
[9]J. H. Lee, L. Fang, E. Vlahos, X. L. Ke, Y. W. Jung, L. F. Kourkoutis, J. W. Kim, P. J. Ryan, T. Heeg, M. Roeckerath, V. Goian, M. Bernhagen, R. Uecker, P. C. Hammel, K. M. Rabe, S. Kamba, J. Schubert, J. W. Freeland, D. A. Muller, C. J. Fennie, P. Schiffer, V. Gopalan, E. Johnston-Halperin, and D. G. Schlom, Nature **466**, 954 (2010).
[10]B. Lorenz, Y. Q. Wang, Y. Y. Sun, and C. W. Chu, Phys. Rev. B **70**, 212412 (2004).
[11]N. Abe, K. Taniguchi, S. Ohtani, H. Umetsu, and T. Arima, Phys. Rev. B **80**, 020402 (2009).
[12]B. Kundys, C. Simon, and C. Martin, Phys. Rev. B **77**, 172402 (2008).

[13]V. R. Palkar, S. C. Purandare, S. Gohil, J. John, and S. Bhattacharya, Appl. Phys. Lett. **90**, 172901 (2007).
[14]A. Kumar, I. Rivera, R. S. Katiyar, and J. F. Scott, Appl. Phys. Lett. **92**, 132913 (2008).
[15]R. Pirc and R. Blinc, Ferroelectrics **400**, 387 (2010).
[16]L. E. Cross, Ferroelectrics **76**, 241 (1987).
[17]J. Dho, W. S. Kim, and N. H. Hur, Phys. Rev. Lett. **89**, 027202 (2002).
[18]L. F. Cotica, S. N. De Medeiros, I. A. Santos, A. Paesano, E. J. Kinast, J. B. M. Da Cunha, M. Venet, D. Garcia, and J. A. Eiras, Ferroelectrics **338**, 241 (2006).
[19]X. Devaux, A. Rousset, J. M. Broto, H. Rakoto, and S. Askenazy, J. Mater. Sci. Lett. **9**, 371 (1990).
[20]L. F. Cotica, I. A. Santos, M. Venet, D. Garcia, J. A. Eiras, and A. A. Coelho, Solid State Commun. **147**, 123 (2008).
[21]G. M. Santos, D. M. Silva, V. F. Freitas, G. S. Dias, A. A. Coelho, M. Pal, I. A. Santos, L. F. Cotica, R. Guo, and A. S. Bhalla, Ferroelectrics **460**, 108 (2014).
[22]F. Bouree, J. L. Baudour, E. Elbadraoui, J. Musso, C. Laurent, and A. Rousset, Acta Crystallogr., Sect. B: Struct. Sci. **52**, 217 (1996).
[23]R. Saha, A. Shireen, S. N. Shirodkar, U. V. Waghmare, A. Sundaresan, and C. N. R. Rao, Solid State Commun. **152**, 1964 (2012).
[24]Y. Shen, J. Gao, Y. Wang, P. Finkel, J. Li, and D. Viehland, Appl. Phys. Lett. **102**, 172904 (2013).
[25]R. Pirc and R. Blinc, Phys. Rev. B **79**, 214114 (2009).
[26]L. F. Cotica, S. C. Zanatta, S. N. de Medeiros, I. A. dos Santos, A. Paesano, and J. B. M. da Cunha, Solid State Ionics **171**, 283 (2004).
[27]Y. Yang, J. Íñiguez, A.-J. Mao, and L. Bellaiche, Phys. Rev. Lett. **112**, 057202 (2014).